The FASEB Journal

FASEB
Federation of American Societies for Experimental Biology

RESEARCH ARTICLE

GLP-1RA Semaglutide Delays the Progression of ADPKD Through Regulation of Glycolysis, Mitochondria Function and Ketosis

Jiao Wu[1,2] | Alice Shasha Cheng[1,3] | Thomas Weimbs[4] | Peter C. Harris[1,3] | Julie Xia Zhou[1,3] | Xiaogang Li[1,3]

[1]Department of Internal Medicine, Mayo Clinic, Rochester, Minnesota, USA | [2]Department of Nephrology, Renhe Hospital, Three Gorges University, Yichang, China | [3]Department of Biochemistry and Molecular Biology, Mayo Clinic, Rochester, Minnesota, USA | [4]Department of Molecular, Cellular, and Developmental Biology, University of California Santa Barbara, Santa Barbara, California, USA

Correspondence: Xiaogang Li (li.xiaogang@mayo.edu)

Received: 14 May 2025 | **Revised:** 16 July 2025 | **Accepted:** 6 August 2025

Funding: This work was supported by HHS | NIH | National Institute of Diabetes and Digestive and Kidney Diseases (NIDDK) (DK129241). HHS | NIH | NIDDK | Division of Diabetes, Endocrinology, and Metabolic Diseases (DEM) (DK126662). U.S. Department of Defense (DOD), (PR221810). American Heart Association (AHA) (24POST1242218). Health Science and Technology Project of China Hubei Province (WJ2025M005).

Keywords: autosomal dominant polycystic kidney disease | glucagon-like peptide-1 | glucose uptake | ketosis | Semaglutide

ABSTRACT

Autosomal dominant polycystic kidney disease (ADPKD) is a genetic disease that is caused by mutations in PKD genes. Glucagon-like peptide-1 (GLP-1) receptor agonists (GLP-1RAs) are a class of medications that mimic the actions of the hormone GLP-1, conferring beneficial effects on weight management and other metabolic conditions. However, whether GLP-1RA plays a kidney-protective action in ADPKD remains unknown. In this study, we define the role and mechanisms of one of the most popular GLP-1RA agonists, Semaglutide, in ADPKD. We show that the expression of GLP-1R is decreased in *Pkd1* mutant renal epithelial cells and kidneys. Treatment with Semaglutide delays cyst growth in aggressive and long-lasting *Pkd1* mutant mouse models. Treatment with Semaglutide (1) decreases glucose uptake, ATP generation, and glycolysis, (2) deactivates PKD-associated signaling pathways, including Rb, S6, and Stat3, resulting in a decrease in cell proliferation, (3) deactivates NF-kB signaling pathways, resulting in a decrease in the expression of cytokines and the recruitment of macrophages, (4) normalizes mitochondrial morphology and function, (5) induces *Pkd1* mutant renal epithelial cell death, (6) induces ketosis characterized by an increase in serum level of beta-hydroxybutyrate (BHB) and the activation of AMPK, and (7) alleviates renal fibrosis through deactivation of TGF-b signaling in *Pkd1* mutant mouse kidneys. This study highlights the potential of GLP-1R agonists as a novel therapeutic strategy for ADPKD treatment.

Abbreviations: ACOX1, acyl-CoA oxidase 1; ADPKD, autosomal dominant polycystic kidney disease; AMPK, adenosine monophosphate protein kinase; ATP, adenosine triphosphate; BHB, beta-hydroxybutyrate; BUN, blood urea nitrogen; cDNA, complementary DNA; CPT1A, carnitine palmitoyltransferase 1A; DAPI, diamidophenylindole; DMSO, dimethylsulfoxide; DPP IV, dipeptidyl-peptidase IV; dUTP, deoxygenation uridine triphosphate; ESRD, end-stage renal disease; FAO, fatty acid oxidation; GLP-1, glucagon-like peptide-1; GLP-1R, glucagon-like peptide-1 receptor; GLP-1RAs, glucagon-like peptide-1 receptor agonists; GPCR, G protein coupled receptor; ht-TKV, height-adjusted total kidney volume; IACUC, institutional animal care and use committee; IHC, histology and immunohistochemistry; IP, intraperitoneal; KO, knockout; KW/BW, kidney weight/body weight; Ldha, lactate dehydrogenase A; Ldhb, lactate dehydrogenase B; MACEs, major adverse cardiovascular events; MCP-1, monocyte chemoattractant protein-1; MEFs, mouse embryonic fibroblasts; MEK, mouse embryonic kidney; MFI, mean fluorescence intensity; NASH, non-alcoholic steatohepatitis; NRK-49F, rat kidney fibroblasts; PKD, polycystic kidney disease; *Pkd1*, polycystic kidney disease 1 gene (Mouse); PN, postnatal; qRT-PCR, quantitative reverse-transcription PCR; ROS, reactive oxygen species; T2DM, type 2 diabetes mellitus; TCA, tricarboxylic acid; TEM, transmission electron microscopy; TGF-β, transforming growth factor-β; TNF-α, tumor necrosis factor alpha; TUNEL, terminal deoxynucleotidyl transferase dUTP nick-end labeling; WT, wild type; α-SMA, alpha smooth muscle actin.

1 | Introduction

Autosomal dominant polycystic kidney disease (ADPKD) is one of the most prevalent genetic disorders characterized by the formation of numerous cysts in kidneys, eventually leading to end-stage renal disease (ESRD) and necessitating dialysis or kidney transplantation for affected patients [1]. The estimated prevalence of ADPKD is approximately 1 in 400 to 1 in 1000 individuals [2]. Current clinical management primarily focuses on symptomatic relief and slowing disease progression, with limited efficacy [3]. The existing treatment, such as tolvaptan, has shown some promise in delaying cyst growth and preserving renal function. However, it is not universally effective and is associated with some kind of adverse effects [4]. Consequently, there is an urgent need for novel therapeutic strategies to improve patient outcomes. Understanding the molecular pathways involved in ADPKD pathogenesis is crucial for the development of effective treatments.

Glucagon like peptide-1 (GLP-1) is a gut-derived peptide hormone deriving from tissue-specific posttranslational processing of the proglucagon peptide, which is produced and released by enteroendocrine L-cells located in the distal jejunum, ileum, and colon in response to nutrient ingestion and neuroendocrine stimulation [5]. GLP-1 plays a pivotal role in the meticulous control of human blood glucose levels [6]. Native GLP-1 has an extremely short half-life, lasting a mere 1–2 min within the circulatory system under typical physiological conditions, due to cleavage by dipeptidyl-peptidase IV (DPP IV) enzymes and renal elimination [7]. The preproglucagon precursor of GLP-1 undergoes enzymatic processing within intestinal L-cells, ultimately giving rise to GLP-1-(1–37) and GLP-1-(7–36) amide or GLP-1 (7–37) peptide variants [8]. The active forms of GLP-1-(7–36) and GLP-1-(7–37) can be cleaved by DPP IV enzymes to produce inactive GLP-1-(9–36) or GLP-1-(9–37), respectively, which have low affinity for their canonical receptor, the GLP-1R [9].

GLP-1R is a member of the (G Protein Coupled Receptor) GPCR family, which exhibits specific affinity for GLP-1 [10]. The GLP-1 receptor is expressed in the pancreas, brain, heart, kidneys, lungs, and stomach but not in the liver, skeletal muscle, or adipose tissue [11]. GLP-1R is predominantly localized on the membrane of diverse cell types and is involved in diverse physiological processes beyond its regulation of glucose metabolism [12]. Knockout (KO) of GLP-1R results in various physiological and metabolic changes, including increased appetite, contributing to weight gain, and impaired insulin and glucagon secretion as well as pancreatic function, affecting the balance of these hormones and glucose homeostasis [13]. Knockout of GLP-1R also has implications for cardiovascular function [14]. Loss of GLP-1R drives a renal phenotype that is accelerated by diabetes [15, 16]. GLP-1 receptor agonists (GLP-1RA) exhibit kidney-protective actions through poorly understood mechanisms.

GLP-1RAs are synthetic protein preparations which exhibit partial or complete amino acid sequence homology with endogenous GLP-1, enabling them to not only replicate the pharmacological functions of GLP-1 but also impede its hydrolysis by DPP IV, thereby resulting in a prolonged half-life and heightened biological activity [17, 18]. GLP-1RAs can effectively lower blood glucose levels without increasing the risk of hypoglycemia and demonstrating favorable safety profiles, which are sanctioned as adjunctive therapies to diet and exercise for the management of type 2 diabetes mellitus (T2DM) in adult patients and potentially hold promise in addressing other medical conditions [19]. It has also been demonstrated that GLP-1 RAs can reduce the risk of major adverse cardiovascular events (MACEs) and have beneficial effects on kidney function in type 2 diabetes patients [15]. The deeper investigation of the multifaceted properties of GLP-1RAs also supports their therapeutic potential across a spectrum of diseases in human populations. For that reason, binding between GLP-1 and its receptor activates adenylate cyclase, which is followed by an increase of cyclic AMP level and cytoplasmic Ca^{2+} [20], two factors that play a critical role in ADPKD; we test the effect of one of the GLP-1RAs, Semaglutide, on cyst progression in ADPKD animal models and elucidate the mechanisms mediated by Semaglutide in ADPKD treatment.

2 | Material and Methods

2.1 | Cell Culture and Reagents

Pkd1 WT and *Pkd1* null MEK cells were maintained as previously described in our recent publications [21]. *Pkd1* heterozygous PH2 cells and homozygous PN24 cells were provided by Stefan Somlo through the George M. O'Brien Kidney Center at Yale University (New Haven, CT, USA) and were cultured according to previously established protocols [22]. NRK-49F cells were cultured at 37°C in 5% CO_2 in DMEM (Invitrogen) supplemented with 10% FBS. Semaglutide was obtained from Cayman (Catalog ID: 29969) and dissolved in DMSO (Sigma-Aldrich) to create a 20 mM stock solution. PN24 cells were treated with Semaglutide for 24 h, after which they were harvested and analyzed by Western blot. Antibodies used for Western blot analysis included (a) anti-GLP-1R (sc-390 774), anti-STAT3 (sc-482), anti-p65 (sc372 and sc-8008), and anti-fibronectin (sc-59 826) antibodies, purchased from Santa Cruz Biotechnology Inc.; (b) anti-S6 (no. 2217), anti-Rb (no. 9309), and the phosphorylated antibodies for S6 (no. 2211), Rb (no. 9307), anti-caspase-3 antibodies (no. 9662), anti-Cleaved caspase-3 antibodies (no. 9661), anti-STAT3-Y705 (no. 9131), anti-p65-S536 (no. 3031) antibodies, purchased from Cell Signaling Technology; (c) anti-α-SMA (ab7817) antibody was purchased from Abcam; (d) anti-actin antibody (A2228) was purchased from Sigma-Aldrich. The secondary antibodies, including donkey anti-rabbit IgG–horseradish peroxidase (sc-2313), donkey anti-goat IgG-horseradish peroxidase (sc-2020), and goat anti-mouse IgG-horseradish peroxidase (sc-2005), were purchased from Santa Cruz Biotechnology Inc.

2.2 | Mouse Strain and Treatment

$Pkd1^{RC/RC}$ mice is a milder hypomorphic ADPKD mouse model with Arg3277Cys (RC) mutation, carrying an arginine (R) to cystine (C) mutation as in ADPKD patients [23]. One-month-old $Pkd1^{RC/RC}$ mice were administered Semaglutide (100 μg/kg) or DMSO via daily intraperitoneal injections from 1 to 3 months of age. Kidneys were harvested from 3-month-old mice for subsequent analysis. $Pkd1^{nl/nl}$ mice is an aggressive hypomorphic *Pkd1* mouse model, yielding only 13%–20% normally spliced *Pkd1* transcripts and resulting

in bilaterally enlarged polycystic kidneys [24]. *Pkd*$^{nl/nl}$ mice were generated by crossbreeding *Pkd1*$^{nl/+}$: *Pkhd1-Cre* females with *Pkd1*$^{n//+}$ males. Neonatal mice were intraperitoneally injected daily with Semaglutide (100 μg/kg) or DMSO from postnatal day 8 (PN8) to PN24, and kidneys were collected and analyzed at PN25. Littermate controls were utilized in all experiments. Both male and female animals were used in all experiments. Statistical analysis was performed in age-matched and sex-matched manners, respectively, and at least three animals of each sex were included. All animal procedures were conducted under IACUC protocol A00003756-R24 (7/26/2024), approved by the Mayo Clinic IACUC, and in compliance with National Institutes of Health, United States Department of Agriculture, and Association for Assessment and Accreditation of Laboratory Animal Care guidelines.

2.3 | Ultrasonic Testing in Mice

All imaging studies were performed on live animals under isoflurane anesthesia. Mice were positioned in dorsal recumbency, and hair removal cream was applied to the abdominal skin to ensure complete hair removal. Coupling gel was then applied to the skin surface to enhance transducer contact. Imaging was conducted using a commercially available ultrasound unit (Vevo 3100, FUJIFILM VisualSonics, Toronto, Ontario, Canada). The MX250s probe was selected for its relatively small footprint, which facilitated better skin contact on the mice. Imaging depth was standardized at 2 cm, and preset gain settings were used to ensure consistency for intermouse image comparison and quantification. Bilateral kidney length, width, and height were recorded to calculate total kidney volumes.

2.4 | Measurement of Cyst Area

Cyst volume was assessed in whole kidneys following H&E staining using Image-Pro Plus v5 software (Media Cybernetics). The cyst area was calculated as (cyst area/total area) × 100%. Three sections from each kidney were analyzed per mouse.

2.5 | Quantitative BUN Determination

To quantitate BUN levels in the mouse blood samples, we used the QuantiChrom TM Urea Assay Kit (BioAssay Systems, DIUR-100). In brief, serum samples were diluted 5-fold with distilled water before the assay. Subsequently, 5 μL of water (blank), 5 μL of standard (50 mg/dL), and 5 μL of sample were pipetted in triplicate into wells of a clear-bottom 96-well plate. Approximately 200 μL of working reagent was added to each well, mixed gently, and the plate was incubated for 20 min at room temperature. Optical density was measured at 520 nm.

2.6 | Western Blot Analysis

Cell pellets were collected and resuspended in lysis buffer composed of 20 mM Tris–HCl (pH 7.4), 150 mM NaCl, 10% glycerol, 1% Triton X-100, 1 mM Na3VO4, 25 mM β-glycerol phosphate, 0.1 mM PMSF, Roche Complete Protease Inhibitor Set, and Sigma-Aldrich Phosphatase Inhibitor Set. The resuspended pellets were vortexed for 20 s, incubated on ice for 30 min, and then centrifuged at 20,000 × *g* for 30 min. The supernatants were collected for Western blot analysis.

2.7 | Histology and Immunohistochemistry (IHC)

Kidneys were fixed in 4% paraformaldehyde (pH 7.4). Paraffin-embedded sections (5 μm) were subjected to H&E, immunohistochemical (IHC) staining, and Picrosirius Red Stain to detect interstitial fibrosis, using the Picrosirius Red Stain Kit (Polysciences Inc) according to the manufacturer's protocol. For GLP-1R staining, a polyclonal rabbit anti-GLP-1R antibody (Santa Cruz Biotechnology Inc.; 1:200 dilution) and a biotinylated secondary antibody (Santa Cruz Biotechnology Inc.; 1:100 dilution) were utilized. Kidney sections were counterstained with hematoxylin. Images were captured and analyzed using a Nikon TI2-E microscope.

2.8 | Immunofluorescence Staining

For GLP-1R staining, a rabbit anti-GLP-1R antibody (Catalog No. sc-390 774, Santa Cruz Biotechnology Inc) and an Alexa Fluor 488 anti-rabbit IgG secondary antibody were employed. Images were analyzed using ImageJ software [25]. Briefly, the 'Split Channels' option was used to separate the color channels into distinct windows, allowing for individual quantitation of each fluorescent channel. An image stained with a nuclear stain was first used to determine the total number of cells in the tissue slice. Subsequently, the GLP-1R staining image was used to measure the mean fluorescence intensity (MFI) in the same tissue slice. The GLP-1R intensity was calculated as the ratio of the MFI to the total number of cells. For Ki67 staining, a rabbit anti-Ki67 antibody (Catalog No. ab15580; Abcam) and an Alexa Fluor 488 anti-rabbit IgG secondary antibody were utilized. Macrophages were detected by immunofluorescence staining using the pan-macrophage marker F4/80. Following antigen retrieval, tissue sections were incubated overnight with a rat anti-mouse F4/80 antibody (Catalog No. 14-4801-82; eBioscience Inc.; 1:100 dilution), then with an Alexa Fluor 555 anti-rat IgG secondary antibody and mounted in ProLong Gold Antifade reagent with DAPI (Invitrogen). For α-SMA staining, a mouse anti-α-SMA antibody and an Alexa Fluor 555 anti-mouse IgG secondary antibody were used. Images were captured and analyzed using a Nikon TI2-E microscope.

2.9 | Transmission Electron Microscopy (TEM)

Kidney tissue samples were fixed in Trump's fixative (pH 7.2) at 4°C overnight; then microwave processed using a Leica EM TP microwave processor: rinsed in phosphate buffer, postfixed in 1% osmium tetroxide, rinsed with distilled water, dehydrated through a graded series of ethanols, further dehydrated with acetone, and infiltrated with epoxy resin via acetone. They were then embedded into pure Spurr resin blocks. The blocks were

cut to 100 nm (or 0.1 μm) ultrathin sections and mounted on 200-mesh copper grids, poststained with lead citrate, and observed under a JEOL JEM-1400 Plus transmission electron microscope at 80 kV.

2.10 | Terminal Deoxynucleotidyl Transferase dUTP Nick-End Labeling (TUNEL) Assay

Kidney sections were analyzed using the TUNEL assay (In Situ Death Detection Kit; Roche Diagnostics, catalog 12156792910), following the manufacturer's protocols. ProLong Gold Antifade reagent with DAPI (Invitrogen) was employed for mounting. Images were captured using a Nikon Eclipse 80i microscope.

2.11 | Quantitative Reverse-Transcription PCR (qRT-PCR)

Total RNA was extracted using either the RNeasy Plus Mini Kit (Qiagen) or Trizol reagents. One microgram of total RNA was used for reverse transcription reactions in a 20-μL volume to synthesize complementary DNA (cDNA) using the iScript cDNA Synthesis Kit (Bio-Rad) or the MicroRNA First-Strand Synthesis Kit (Takara Bio). RNA or miRNA expression profiles were analyzed by real-time PCR employing iTaq SYBR Green Supermix with ROX (Bio-Rad) on an iCycler iQ Real-Time PCR Detection System. The PCR protocol consisted of 40 cycles of 10 s at 95°C and 20 s at 60°C, followed by a melting curve analysis and a cooling step. Each sample was assayed in triplicate, and experiments were conducted in triplicate as well. Target gene expression levels were normalized to the expression level of actin. The sequences of all primers used in this study are listed in Table S1.

2.12 | Quantitative BHB Determination

The beta-hydroxybutyrate level was evaluated using BHB-GloTM (Ketone Body) Assay Kit (Promega, JE9500) according to the manufacturer's instructions. Briefly, serum and 4 μM BHB spike were diluted in PBS. Then, 10 μL of 0.6 N HCl was added, then incubated for 5 min. 10 μL of neutralization buffer was added to the above solution and shaken for 30–60 s, then the BHB detection reagent was added. Finally, the luminescence signal was recorded after being incubated at room temperature for 60 min. BHB concentration in the serum sample can be calculated using the following formula based on the instructions of this Kit.

$$\{\mathrm{BHB}\} = \{\mathrm{BHB\ standard}\}\ (\mu\mathrm{M}) \times \left(\mathrm{RLU}_{\mathrm{sample}} - \mathrm{RLU}_{\mathrm{background}}\right) \left(\mathrm{RLUBHB}_{\mathrm{standard}} - \mathrm{RLU}_{\mathrm{background}}\right)$$

2.13 | Statistics

Data are presented as mean ± SEM. Statistical analyses were performed using GraphPad Prism version 10. *P*-values were determined using unpaired Two-tailed *t* test and one-way ANOVA, with a *p*-value <0.05 considered statistically significant.

2.14 | Study Approval

All animal procedures were approved by the Laboratory Animal Resources of Mayo Clinic and conducted in accordance with Institutional Animal Care and Use Committee regulations.

3 | Results

3.1 | The Expression of GLP-1R Was Downregulated in Cystic Kidneys

To determine the role of GLP-1R in ADPKD, we investigated the expression of GLP-1R in *Pkd1* mutant renal epithelial cells and tissues. We found that the expression of GLP-1R was decreased in *Pkd1* null mouse embryonic kidney (MEK) cells and postnatal *Pkd1* homozygous PN24 cells compared with *Pkd1* wild type (WT) MEK cells and postnatal *Pkd1* heterozygous PH2 cells, as well as in kidneys from $Pkd1^{RC/RC}$ mice and $Pkd1^{nl/nl}$ mice, two hypomorphic ADPKD mouse models [26, 27], compared with age-matched controls as analyzed with Western blots (Figure 1A–C) and quantitative reverse transcription PCR (qRT-PCR) (Figure 1D–G). The expression of GLP-1R was also decreased in the cyst-lining epithelial cells of *Pkd1* mutant mouse kidneys compared to that in normal kidneys as examined with immunohistochemistry (IHC) staining (Figure 1H,I).

3.2 | Treatment With a GLP-1 Receptor Agonist, Semaglutide, Delays Cyst Growth in *Pkd1* Mutant Mouse Kidneys

For the downregulation of GLP-1R in cystic renal epithelial cells and tissues, we investigated whether treatment with the GLP-1 receptor agonist, Semaglutide, affected cyst growth in vivo. We first treated $Pkd1^{RC/RC}$ mice, a slowly progressive *Pkd1* hypomorphic mouse model [26], with Semaglutide (100 ug/kg) ($n = 10$) or vehicle ($n = 10$) by intraperitoneal (IP) injection three times a week from postnatal day 30 (PN30) to PN90 and collected kidneys at PN91 (Figure 2A). The dosage, route, and timing of Semaglutide administration to *Pkd1* mutant mice were based on previous publications [28, 29]. The height-adjusted total kidney volume (ht-TKV) was analyzed with ultrasound at PN60; we found that treatment with Semaglutide decreased the ht-TKV in $Pkd1^{RC/RC}$ mice compared with age-matched controls treated with vehicle (Figure 2B,C). We also found that treatment with Semaglutide ($n = 10$) delayed cyst growth as seen by a decrease of the cystic index (Figure 2D,E), kidney weight/body weight (KW/BW) ratios (Figure 2F) and blood urea nitrogen (BUN) levels (Figure 2G) in PN91 $Pkd1^{RC/RC}$ mice compared to age-matched $Pkd1^{RC/RC}$ mice treated with vehicle. In addition, treatment with Semaglutide decreased cyst-lining epithelial cell proliferation as examined by Ki67 staining (Figure 2H), but induced cyst-lining epithelial cell apoptosis as examined by terminal deoxynucleotidyl transferase dUTP nick-end labeling (TUNEL) assay

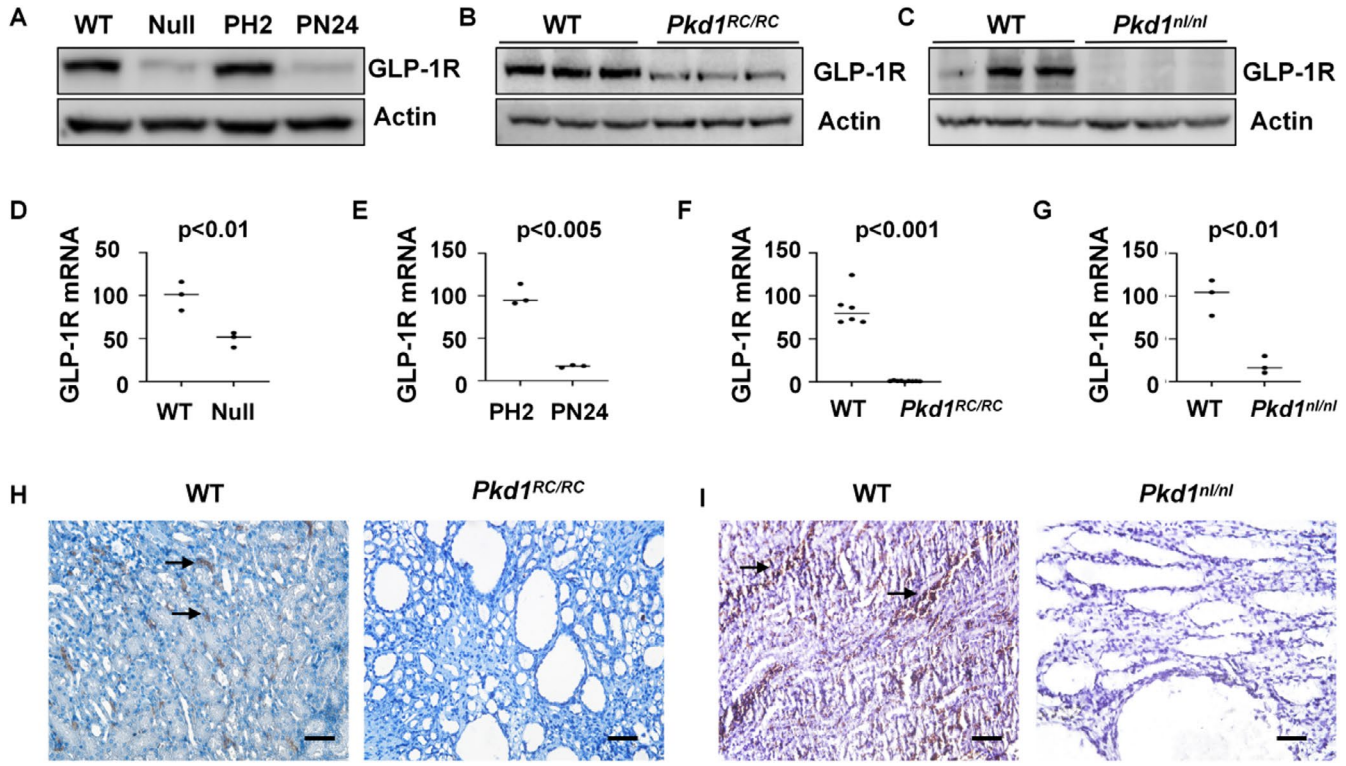

FIGURE 1 | The expression of GLP-1R is decreased *Pkd1* mutant renal epithelial cells and tissues. (A) Western blot analysis of the protein expression of GLP-1R from whole-cell lysates of *Pkd1* wild type (WT) and $Pkd1^{null/null}$ (Null) MEK cells, as well as in postnatal *Pkd1* heterozygous PH2 (PH2) cells and *Pkd1* homozygous PN24 (PN24) cells. (B) Western blot analysis of the protein expression of GLP-1R in 3-month-old kidneys from $Pkd1^{RC/RC}$ mice compared to WT mice. (C) Western blot analysis of the protein expression of GLP-1R in PN25 kidneys from $Pkd1^{nl/nl}$ mice compared to $Pkd1^{nl/+}$ (WT) mice. (D) qRT-PCR analysis of the expression of GLP-1R mRNA in *Pkd1* WT and $Pkd1^{null/null}$ (Null) MEK cells ($p < 0.01$). (E) qRT-PCR analysis of the expression of GLP-1R mRNA in postnatal *Pkd1* heterozygous PH2 (PH2) cells and *Pkd1* homozygous PN24 (PN24) cells ($p < 0.005$). (F) qRT-PCR analysis of the expression of GLP-1R mRNA in kidneys from 3-month-old $Pkd1^{RC/RC}$ mice compared to that in kidneys from age matched WT mice ($p < 0.01$). $n = 3$. (G) qRT-PCR analysis of the expression of GLP-1R mRNA in PN25 $Pkd1^{nl/nl}$ mice ($p < 0.01$) compared to that in kidneys from age matched WT mice. $n = 3$. Statistical analysis was performed using an unpaired two-tailed *t* test. (H and I) GLP-1R expression was decreased in cyst-lining epithelial cells in *Pkd1* mutant kidneys as examined by Histology and immunohistochemistry (IHC) with anti-GLP-1R antibody in 3-month-old kidneys from WT and $Pkd1^{RC/RC}$ mice (H), as well as in PN25 kidneys from WT and $Pkd1^{nl/nl}$ mice (I). Scale bars: 100 μm.

(Figure 2I) in kidneys of $Pkd1^{RC/RC}$ mice. Because it has been reported that treatment with Semaglutide may affect weight loss and blood glucose level [30–32], we monitored body weight and blood glucose levels in $Pkd1^{RC/RC}$ mice treated with Semaglutide and vehicle (DMSO). We found that treatment with Semaglutide for 2 months exhibited a decrease in body weight (Figure 2J), but had no significant effect on blood glucose levels in $Pkd1^{RC/RC}$ mice compared to age-matched controls (Figure 2K).

We also treated early stage $Pkd1^{nl/nl}$ mice, another hypomorphic *Pkd1* mouse model with more rapidly progressive cyst development [27], with Semaglutide (100ug/kg) ($n = 8$) or vehicle ($n = 8$) by intraperitoneal injection three times a week from postnatal day 8 (PN8) to PN24 and sacrificed the mice at PN25. Treatment with Semaglutide also decreased cyst growth in $Pkd1^{nl/nl}$ mice as seen by a decrease of cystic index (Figure S1A,B), KW/BW (Figure S1C) and BUN levels (Figure S1D), as well as cyst lining epithelial cell proliferation as examined with Ki67 staining (Figure S1E), and an induction of cyst-lining epithelial cell apoptosis as examined with TUNEL assay (Figure S1F) in kidneys from $Pkd1^{nl/nl}$ mice compared to those in age-matched $Pkd1^{nl/nl}$ mice treated with vehicle. Treated with Semaglutide exhibited a decrease of body weight (Figure S1G) but had no significant effect on blood glucose levels (Figure S1H) in $Pkd1^{nl/nl}$ mice. These results suggest that treatment with Semaglutide may delay cyst growth in ADPKD patients.

3.3 | Treatment With Semaglutide Decreases Glucose Uptake, ATP Generation, and Glycolysis in *Pkd1* Mutant Renal Epithelial Cells and Tissues

Semaglutide has been reported to regulate glucose uptake and reduce glycolytic processes in various metabolic diseases [33]. Deprivation of glucose abrogated the higher ATP content of *Pkd1* mutant mouse embryonic fibroblasts (MEFs), and glucose addition increased the intracellular ATP in these cells [34, 35]. We found that treatment with Semaglutide decreased the uptake of glucose (Figure 3A,B) and the levels of intracellular ATP in *Pkd1* mutant renal epithelial cells (Figure 3C,D). In addition, treatment with Semaglutide decreased the mRNA level of the key glycolytic enzymes Hk1, Pkm2, Ldha, and Ldhb in *Pkd1* null MEK and PN24 cells (Figure S2A,B).

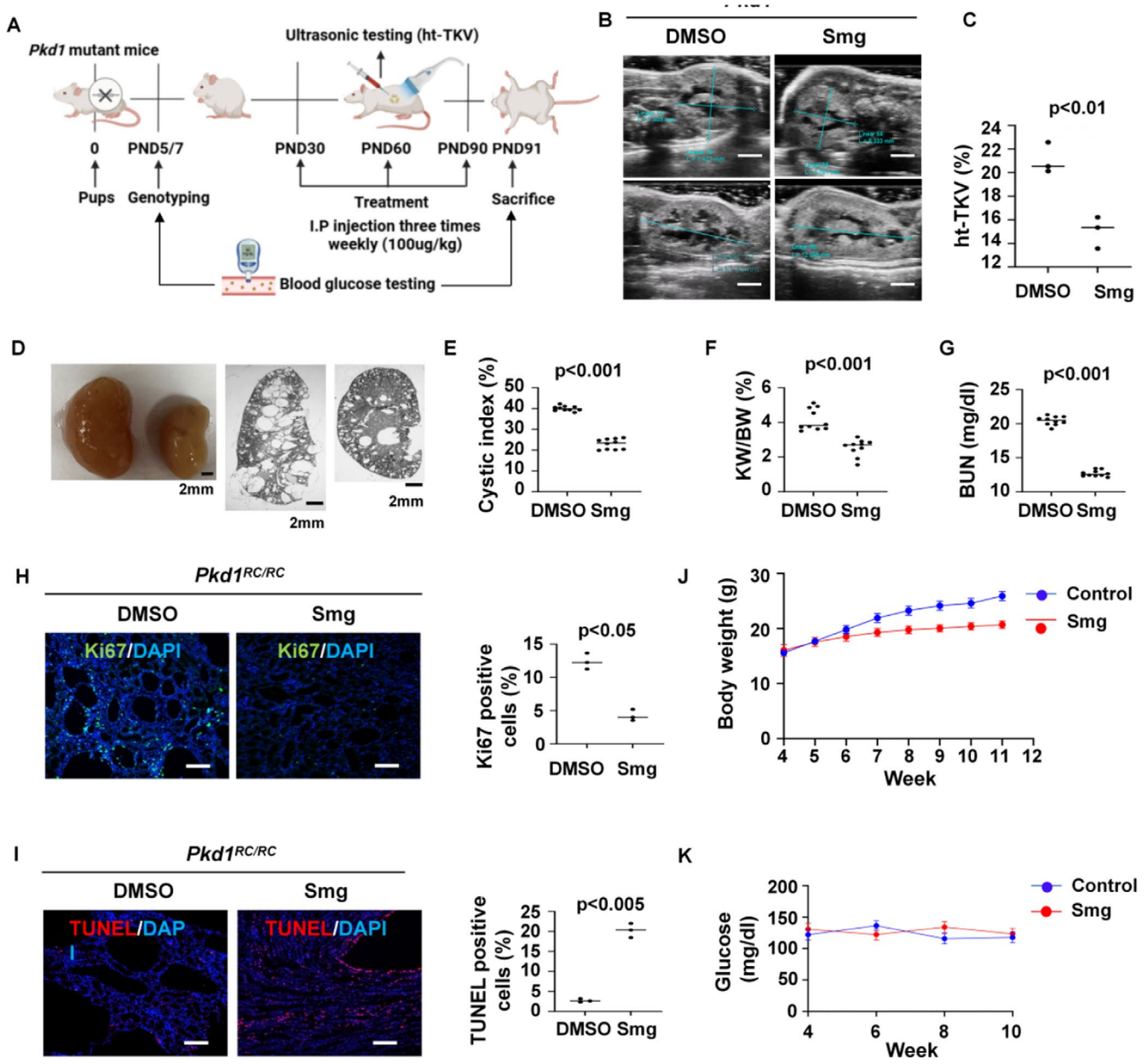

FIGURE 2 | Treatment with GLP-1RA, Semaglutide, delays cyst growth in *Pkd1*$^{RC/RC}$ mouse kidneys. (A) Protocol of the treatment with GLP-1RA Semaglutide to the *Pkd1*$^{RC/RC}$ mice. (B) Ultrasound examination of PN60 kidneys from *Pkd1*$^{RC/RC}$ mice treated with vehicle (DMSO) ($n=3$) or Semaglutide ($n=3$). Scale bar: 2 mm. (C) Kidney height-to-total kidney volume (ht-TKV) ratios were decreased in PN60 kidneys from *Pkd1*$^{RC/RC}$ mice treated with Semaglutide ($n=3$) compared with mice treated with DMSO ($n=3$). $p<0.01$. (D) Histologic examination of PN91 kidneys from *Pkd1*$^{RC/RC}$ mice treated with vehicle (DMSO) ($n=10$) or Semaglutide ($n=10$). Scale bar: 2 mm. (E) Quantification of the percentage of cystic areas over total kidney-section areas of PN91 kidneys from *Pkd1*$^{RC/RC}$ mice treated as in A. Shown is mean ± SEM of all sections quantified for each condition. $p<0.001$. (F and G) Kidney weight-to-body weight (KW/BW) ratios (F) and blood urea nitrogen (BUN) levels (G) were decreased in PN91 kidneys from *Pkd1*$^{RC/RC}$ mice treated with Semaglutide compared with mice treated with DMSO (control). $p<0.01$. (H) Semaglutide treatment reduced cyst-lining epithelial cell proliferation in kidneys from *Pkd1*$^{RC/RC}$ mice, as detected with Ki67 staining. The percentage of Ki67-positive nuclei in cystic epithelial cells was calculated from an average of 1000 nuclei per mouse kidney section. It was calculated as Ki67 positive cyst-lining epithelial cells/total cyst-lining epithelial cells ×100%, and five images of each animal were counted, $n=3$ animals were scored. $p<0.05$. Scale bars: 100 μm. (I) Semaglutide treatment induced cyst-lining epithelial cell death in kidneys from *Pkd1*$^{RC/RC}$ mice as detected by TUNEL assay. It was calculated as TUNEL-positive cyst-lining epithelial cells/total cyst-lining epithelial cells ×100%, and five images of each animal were counted, $n=3$ animals were scored. $p<0.005$. Scale bars: 100 μm. (J) Semaglutide treatment attenuated the rate of body weight gain in *Pkd1*$^{RC/RC}$ mice relative to vehicle controls, as assessed by weekly measurements. (K) The blood glucose in *Pkd1*$^{RC/RC}$ mice treated with Semaglutide compared to DMSO has no statistical difference as detected every week after treated with Semaglutide or DMSO. Statistical analysis was performed using an unpaired two-tailed Student's *t* test.

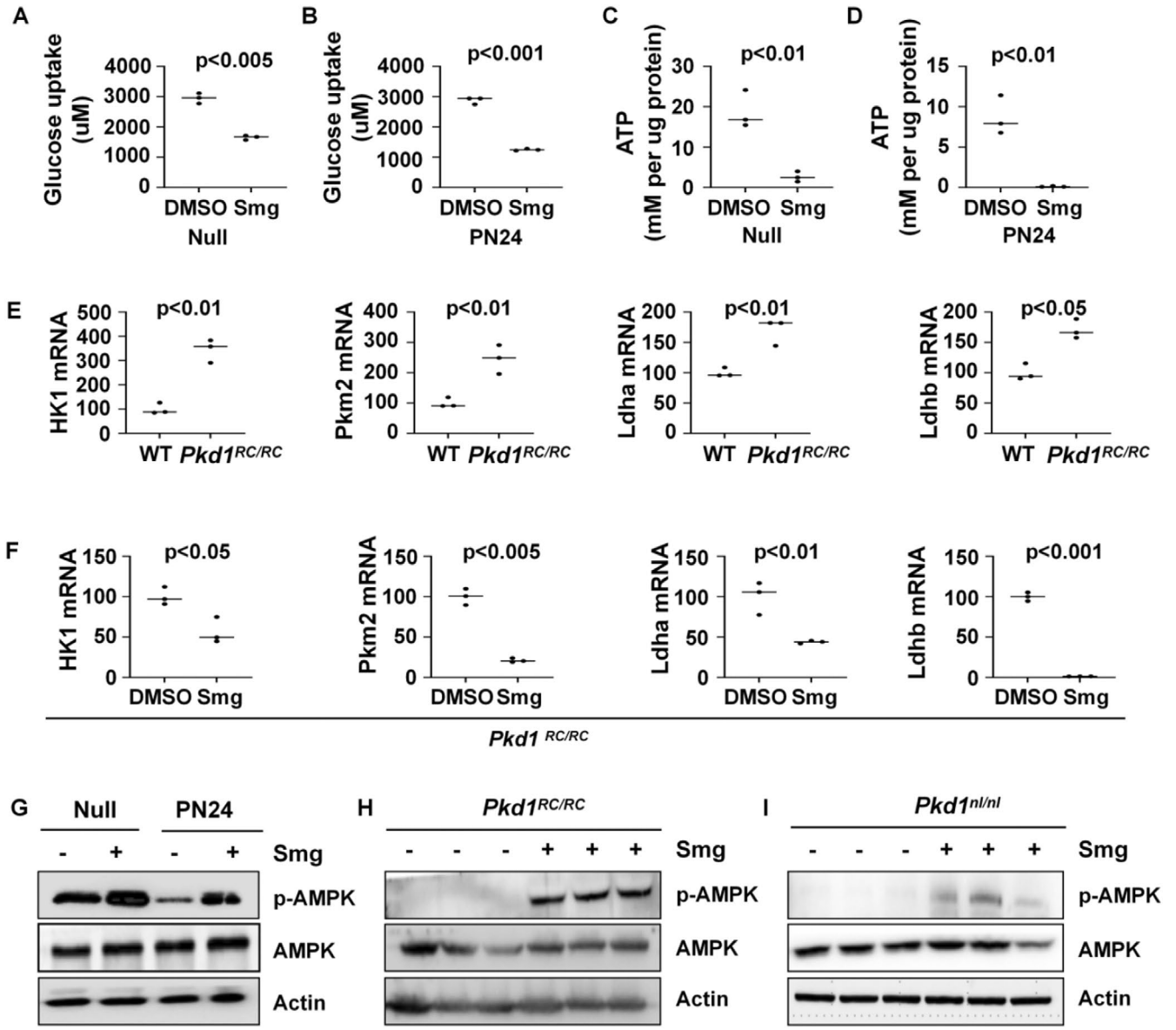

FIGURE 3 | Treatment with Semaglutide decreases glucose uptake, ATP generation and glycolysis in *Pkd1* mutant renal epithelial cells and tissues. (A) Treatment with Semaglutide decreased the uptake of glucose in *Pkd1* null MEK cells compared with untreated *Pkd1* mutant MEK cells. $n = 3$, $p < 0.005$; two-tailed unpaired *t* tests. (B) Treatment with Semaglutide decreased the uptake of glucose in *Pkd1* homozygous PN24 cells compared with untreated *Pkd1* homozygous PN24 cells. $n = 3$, $p < 0.001$. (C) Treatment with Semaglutide decreased the levels of intracellular ATP in *Pkd1* null MEK cells compared with untreated *Pkd1* null MEK cells. $n = 3$, $p < 0.01$. (D) Treatment with Semaglutide decreased the levels of intracellular ATP in *Pkd1* homozygous PN24 cells. (E) qRT-PCR analysis of the expression of *Hk1*, *Pkm2*, *Ldha* and *Ldhb* mRNA in kidneys from 3-month-old kidneys from WT and $Pkd1^{RC/RC}$ mic. $n = 3$, $p < 0.05$. (F) qRT-PCR analysis of the expression of *Hk1*, *Pkm2*, *Ldha* and *Ldhb* mRNA in PN90 kidneys from $Pkd^{RC/RC}$ mice treated with Semaglutide or DMSO. $n = 3$, $p < 0.05$. (G–I) Western blot analysis of the expression of p-AMPK and AMPK in *Pkd1* mutant MEK cells and *Pkd1* homozygous PN24 cells (G), $Pkd1^{RC/RC}$ (H) and $Pkd1^{nl/nl}$ kidneys (I) treated with Semaglutide and vehicle. The levels of p-AMPK and AMPK were increased in *Pkd1* mutant MEK cells and *Pkd1* homozygous PN24 cells, $Pkd1^{RC/RC}$ and $Pkd1^{nl/nl}$ kidneys treated with Semaglutide compared to vehicle DMSO. Statistical analysis was performed using an unpaired Two-tailed Student's *t* test.

We further found that the mRNAs of *Hk1, Pkm2, Ldha*, and *Ldhb* were increased in kidneys from $Pkd1^{RC/RC}$ mice compared with age-matched WT mice, as examined by qRT-PCR; whereas treatment with Semaglutide decreased the mRNAs of these key glycolytic genes (Figure 3E,F). To elucidate the mechanism of how Semaglutide affected glycolysis in *Pkd1* mutant renal epithelial cells and tissues, we found that treatment with Semaglutide increased the phosphorylation of AMPK in *Pkd1* mutant renal epithelial cells and tissues, as examined with Western blot analysis (Figure 3G–I). It has been reported that the phosphorylation/activation of AMPK plays a significant role in regulating glycolysis through (1) directly influencing enzymes involved in glycolysis and (2) indirectly affecting other metabolic pathways and transcription factors, such as inhibition of mTORC1, a key driver of cyst growth [36, 37]. These results suggest that Semaglutide may regulate

glucose uptake and ATP production through the activation of AMPK signaling, as being reported [38].

3.4 | Treatment With Semaglutide Normalizes Mitochondrial Morphology and Function in *Pkd1* Mutant Mouse Kidneys

Mitochondria are the energy center of the kidney, and dynamic mitochondrial fusion and division regulate fuel oxidative phosphorylation and the intracellular ATP supply in renal epithelial cells [39]. Mitochondrial respiratory chain proteins guarantee the production of ATP [40]. We found that the expression of mitochondrial respiratory chain-related genes, including mt-Nd6, mt-Col1, mt-Cytb, and mt-Rnr2, was decreased in *Pkd1* mutant renal epithelial cells and kidneys (Figure S3A,B); whereas treatment with Semaglutide could normalize the expression of these genes in *Pkd1* mutant renal epithelial cells and kidneys (Figure 4A,B). With transmission electron microscopy (TEM), we observed that the administration of Semaglutide restored the swelling of the mitochondrial matrix and the shortening and reduction of cristae in *Pkd1*

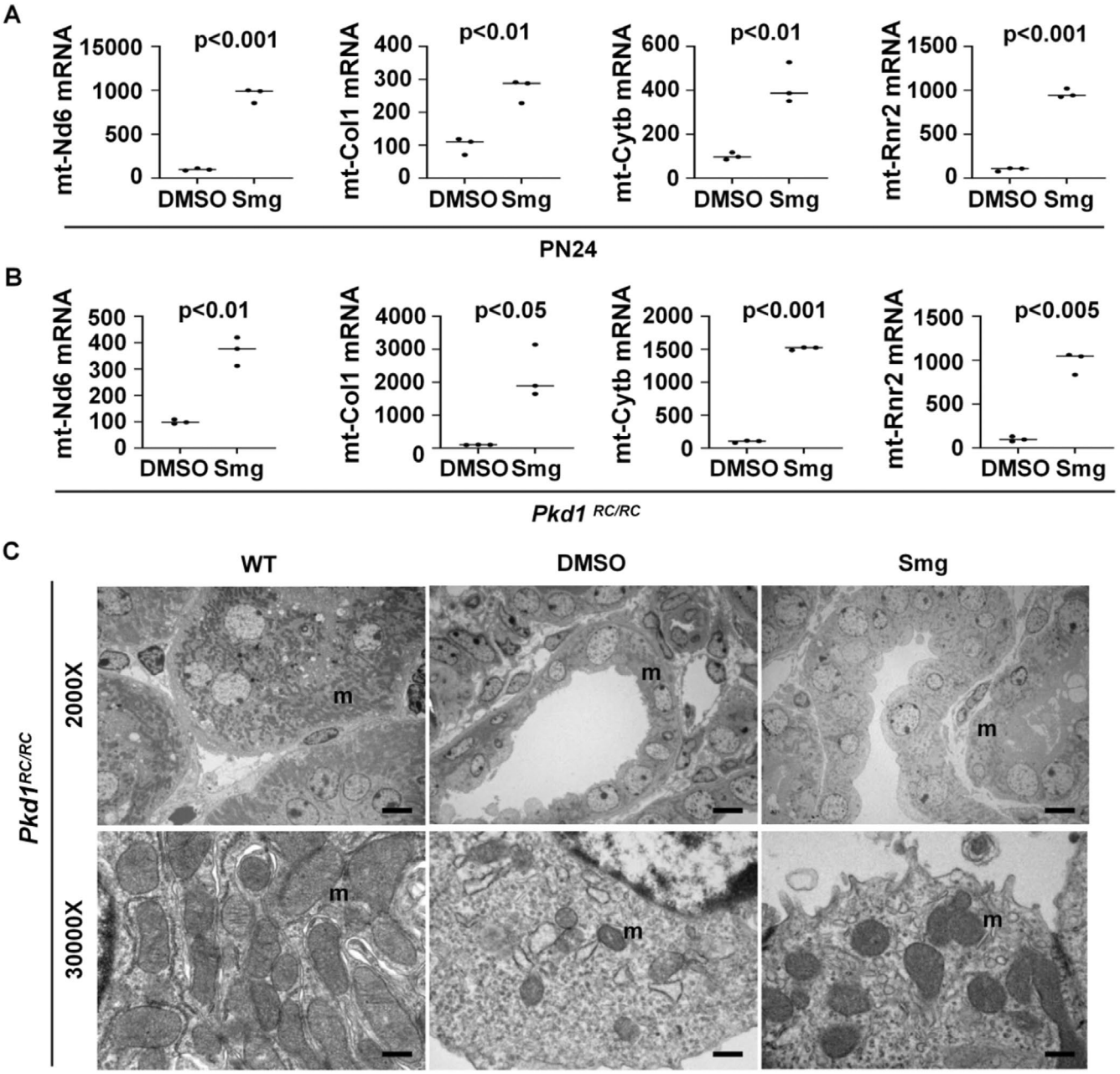

FIGURE 4 | Treatment with Semaglutide normalizes mitochondrial fusion and morphology in *Pkd1* mutant kidneys. (A and B) Relative mRNA levels of mitochondrial oxidative phosphorylation (OXPHOS) associated genes, including mt-Nd6, mt-Co1, mt-Cytb, mt-Rnr2, were increased in *Pkd1* homozygous PN24 cells (A) and $Pkd1^{RC/RC}$ kidneys (B) after being treated with Semaglutide compared to vehicle (DMSO) treated controls (C) $p < 0.05$. Statistical analysis was performed using an unpaired two-tailed Student's *t* test. (C) Transmission electron micrographs (TEM) analysis demonstrated that the morphology of mitochondria (m) was changed in renal epithelia cells in $Pkd1^{RC/RC}$ kidneys compared to that in age matched WT kidneys, and treatment with Semaglutide leads to a normalization of these changes in $Pkd1^{RC/RC}$ kidneys. Scale bars: 200 μm.

mutant renal epithelial cells in *Pkd1*$^{RC/RC}$ (Figure 4C) and *Pkd1*$^{nl/nl}$ (Figure S4) kidneys. In addition, the reduction of the abundance of mitochondria was restored in Semaglutide-treated *Pkd1* mutant kidneys (Figure 4C; Figure S4). These results suggest that treatment with Semaglutide can normalize the morphology and function of mitochondria in ADPKD kidneys.

3.5 | Treatment With Semaglutide Normalizes PKD Associated Signaling Pathways That Contribute to *Pkd1* Mutant Renal Epithelial Cell Proliferation; Induces Cell Death Characterized by an Increase of the Cleavage of Caspase 3

We found that treatment with Semaglutide decreased the phosphorylation of Rb, S6, and Stat3 in *Pkd1* mutant mouse embryonic kidney (MEK) cells and postnatal *Pkd1* homozygous PN24 cells compared with *Pkd1* WT MEK cells and postnatal *Pkd1* heterozygous PH2 cells (Figure 5A), as well as in kidneys from *Pkd1*$^{RC/RC}$ mice and *Pkd1*$^{nl/nl}$ mice compared with age-matched controls treated with vehicle, as examined with Western blot analysis (Figure 5B,C). We also found that treatment with Semaglutide increased the cleavage of caspase 3 (Figure 5D–F). These results suggest that Semaglutide can regulate multiple PKD-associated signaling pathways to inhibit cystic epithelial cell proliferation and induce cell death.

3.6 | Treatment With Semaglutide Decreases the Expression of Cytokines and the Recruitment of Macrophages in *Pkd1* Mutant Kidneys and Cells

It has been reported that a substantial recruitment of macrophages to interstitial and pericyclic regions promotes cyst growth in orthologous ADPKD mouse models [41–43]. Cytokines, such as TNF-α and MCP-1, play crucial roles in the recruitment of macrophages and renal inflammation in cystic kidneys [41, 43]. We found that treatment with Smaglutide decreased the recruitment of macrophages in *Pkd1* mutant kidneys compared to that in age-matched control mice treated with vehicle as analyzed with F4/80 staining (Figure 5A,B). In addition, treatment with Smaglutide decreased TNF-α and MCP-1 mRNAs in *Pkd1* null MEK cells and PN24 cells, as well as in *Pkd1*$^{RC/RC}$ kidneys as examined with qRT-PCR analysis (Figure S5C–H). The expression of TNF-α and MCP-1 can be regulated by NF-kB signaling [43, 44]. We found that treatment with Semaglutide decreased the phosphorylation of the p65 subunit of NF-kB in *Pkd1* null MEK cells and PN24 cells as well as in *Pkd1*$^{RC/RC}$ and *Pkd1*$^{nl/nl}$ kidneys as examined with western blot analysis (Figure 6A–C).

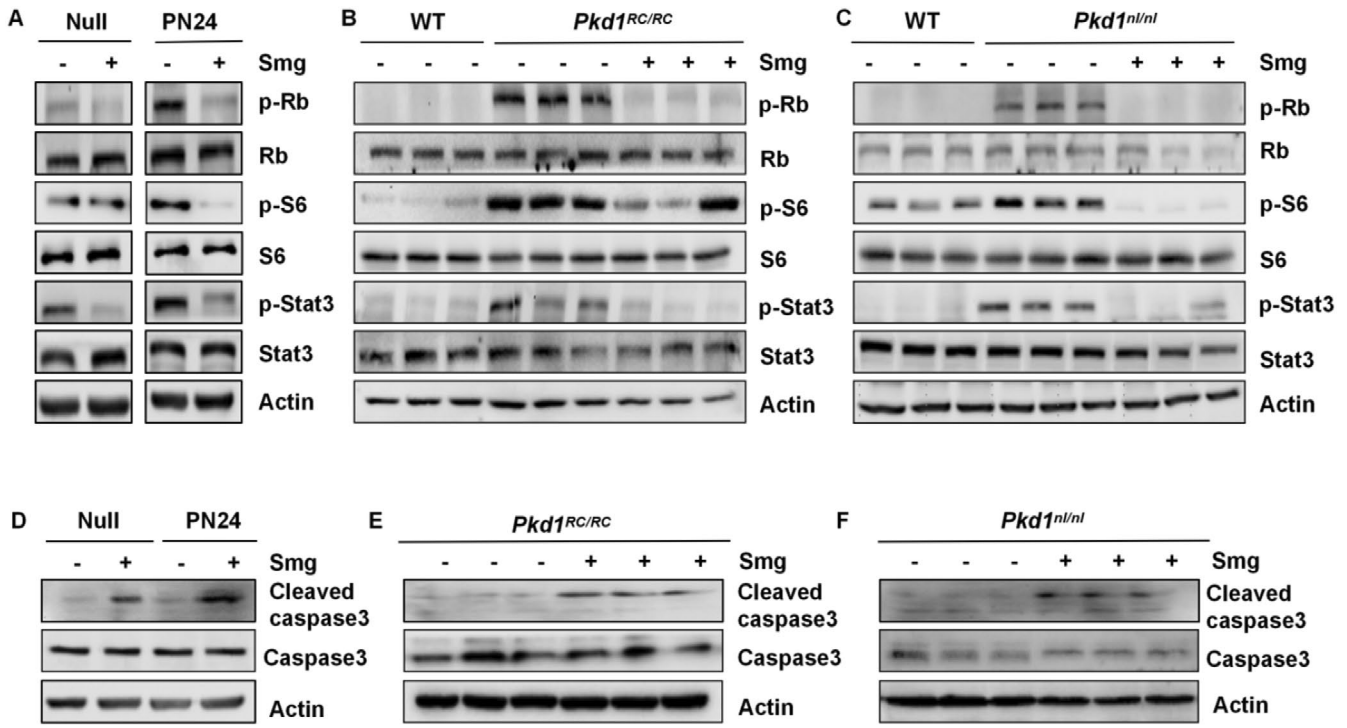

FIGURE 5 | Treatment with Smgalutide decreases *Pkd1* mutant renal epithelial cell proliferation and induces cell death in *Pkd1* mutant kidneys. (A) Western blot analysis of the expression of p-Rb, Rb, p-S6, S6, p-Stat3 and Stat3 in *Pkd1* mutant MEK Null cells and *Pkd1* homozygous PN24 cells treated with Semaglutide or vehicle DMSO. (B, C) Western blot analysis of the expression of p-Rb, Rb, p-S6, S6, p-Stat3 and Stat3 in kidneys from PN91 *Pkd1*$^{RC/RC}$ mice (B) and PN25 *Pkd1*$^{nl/nl}$ mice (C) treated with Semaglutide or vehicle DMSO, as well as in kidneys from age matched WT mice. (D) Western blot analysis of the expression of Cleaved caspase3 and Caspase3 in *Pkd1* mutant MEK Null cells and *Pkd1* homozygous PN24 cells treated with Semaglutide or vehicle DMSO. (E, F) Western blot analysis of the expression of cleaved caspase3 and caspase3 in kidneys from PN91 *Pkd1*$^{RC/RC}$ mice (E) and PN25 *Pkd1*$^{nl/nl}$ mice (F) treated with semaglutide or vehicle DMSO.

These results suggest that treatment with Smaglutide decreases cytokine expression and macrophage recruitment through NF-κB signaling in *Pkd1* mutant kidneys.

3.7 | Treatment With Semaglutide Induces Ketosis Characterized by an Increase of Serum Levels of Beta-Hydroxybutyrate (BHB) in *Pkd1* Mutant Mice

It has been reported that mild reduction in food intake slows PKD progression in mouse models due to an induction of ketosis, a process that happens when the body does not have enough carbohydrates to burn for energy [45]. To detect the effect of Semaglutide on ketosis in ADPKD, we evaluated whether treatment with Semaglutide affects the serum level of beta-hydroxybutyrate (BHB), an important index of ketosis. We found that the level of BHB was decreased in the serum of 3-month-old $Pkd1^{RC/RC}$ mice compared to that in the serum of aged matched wild-type mice, whereas treatment with Semaglutide could increase the BHB levels in the serum of $Pkd1^{RC/RC}$ mice (Figure 6A). BHB can regulate AMPK activation through its interaction with the G-protein-coupled receptor GPR109A [46]. We found that treatment with either Semaglutide or BHB increased the phosphorylation of AMPK, and the co-treatment with Semaglutide plus BHB further increased the phosphorylation of AMPK in *Pkd1* null MEK and PN24 cells (Figure 6B). In addition, it has been reported that AMPK activation leads to an increase in fatty acid oxidation (FAO), which is regulated by two key enzymes, carnitine palmitoyltransferase 1A (CPT1A) and acyl-CoA oxidase 1 (ACOX1) [47, 48], ultimately promoting energy production [49]. Overexpression of CPT1A and ACOX1 can restore mitochondrial homeostasis [50, 51]. We found that treatment with Semaglutide increased the transcription of CPT1A (Figure 6C–E) and ACOX1 (Figure 6F–H) in *Pkd1* null MEK and PN24 cells as well as in $Pkd1^{RC/RC}$ mouse kidneys as detected by qRT-PCR analysis. These results suggest that a potential mechanism of Semaglutide treatment in delaying cyst growth is through induction of ketosis characterized by an increase in serum BHB level and the activation of AMPK in *Pkd1* mutant cells and kidneys.

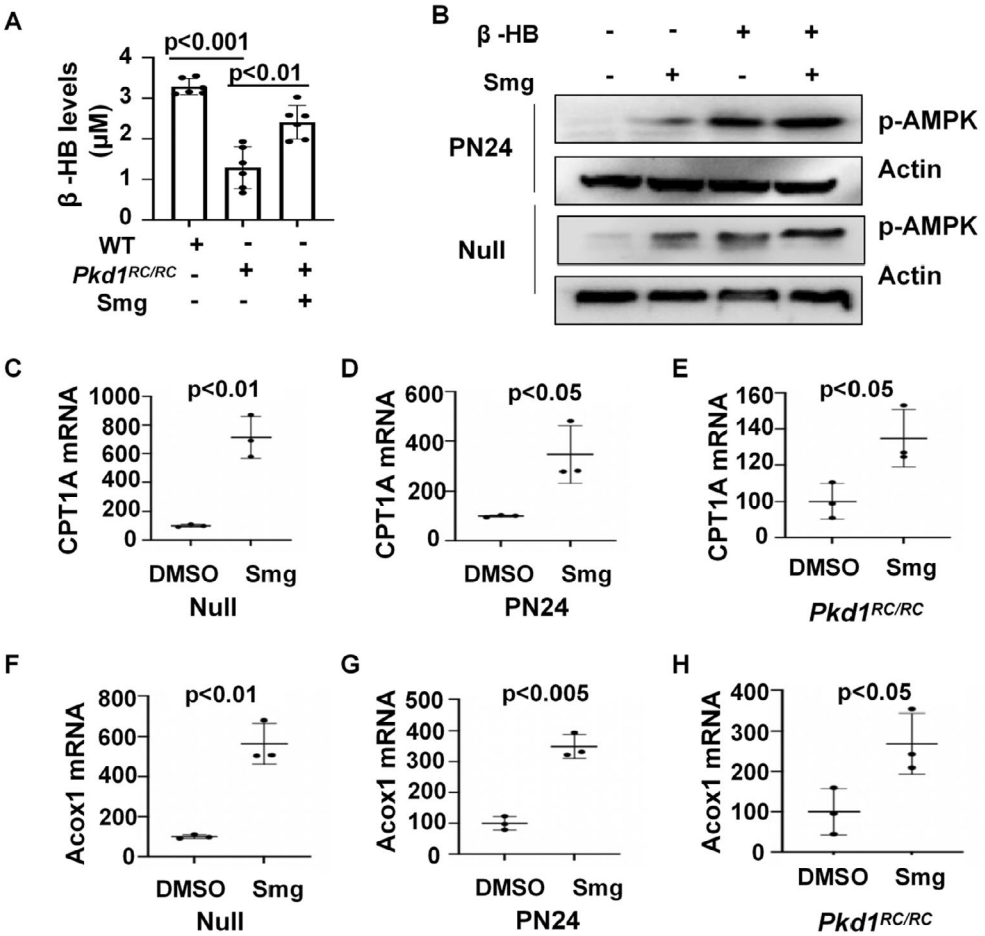

FIGURE 6 | Treatment with Smgalutide increases serum BHB level and the activation of AMPK *Pkd1* mutant r kidneys. (A) β-HB levels in the serum of 3-month-old WT, $Pkd1^{RC/RC}$ as well as Semaglutide treatment group. $n = 6$. Statistical analysis was performed using an unpaired two-tailed Student's *t* test. (B) Western blot analysis of p-AMPK in *Pkd1* mutant renal epithelial cells treated with Smaglutide, BHB, as well as Smaglutide plus BHB. (C–E) qRT-PCR analysis of relative *CPT1A* mRNA expression in Null and PN24 cells, and $Pkd1^{RC/RC}$ and age matched wild type (WT) kidneys. $n = 3$. (F–H) qRT-PCR analysis of relative *ACOX1* mRNA expression in Null and PN24 cells, and $Pkd1^{RC/RC}$ and age matched WT kidneys. $n = 3$. Statistical analysis was performed using an unpaired two-tailed Student's *t* test.

3.8 | Treatment With Semaglutide Alleviates Renal Fibrosis in *Pkd1* Mutant Mouse Kidneys

Renal fibrosis represents a final outcome leading to end-stage renal failure in ADPKD [52]. We found that treatment with Smaglutide decreased the expression of fibrotic markers, including fibronectin and alpha smooth muscle actin (α-SMA), in kidneys from $Pkd1^{RC/RC}$ or $Pkd1^{nl/nl}$ mice compared with vehicle-treated control mice as examined with western blot analysis (Figure 7A,B). In addition, treatment with Smaglutide decreased the expression of fibronectin and α-SMA in rat kidney fibroblasts (NRK-49F) after induction with TGF-β compared to those cells treated with vehicle (Figure 7C). The mRNA levels of TGF-β, α-SMA, and Col1 were also decreased

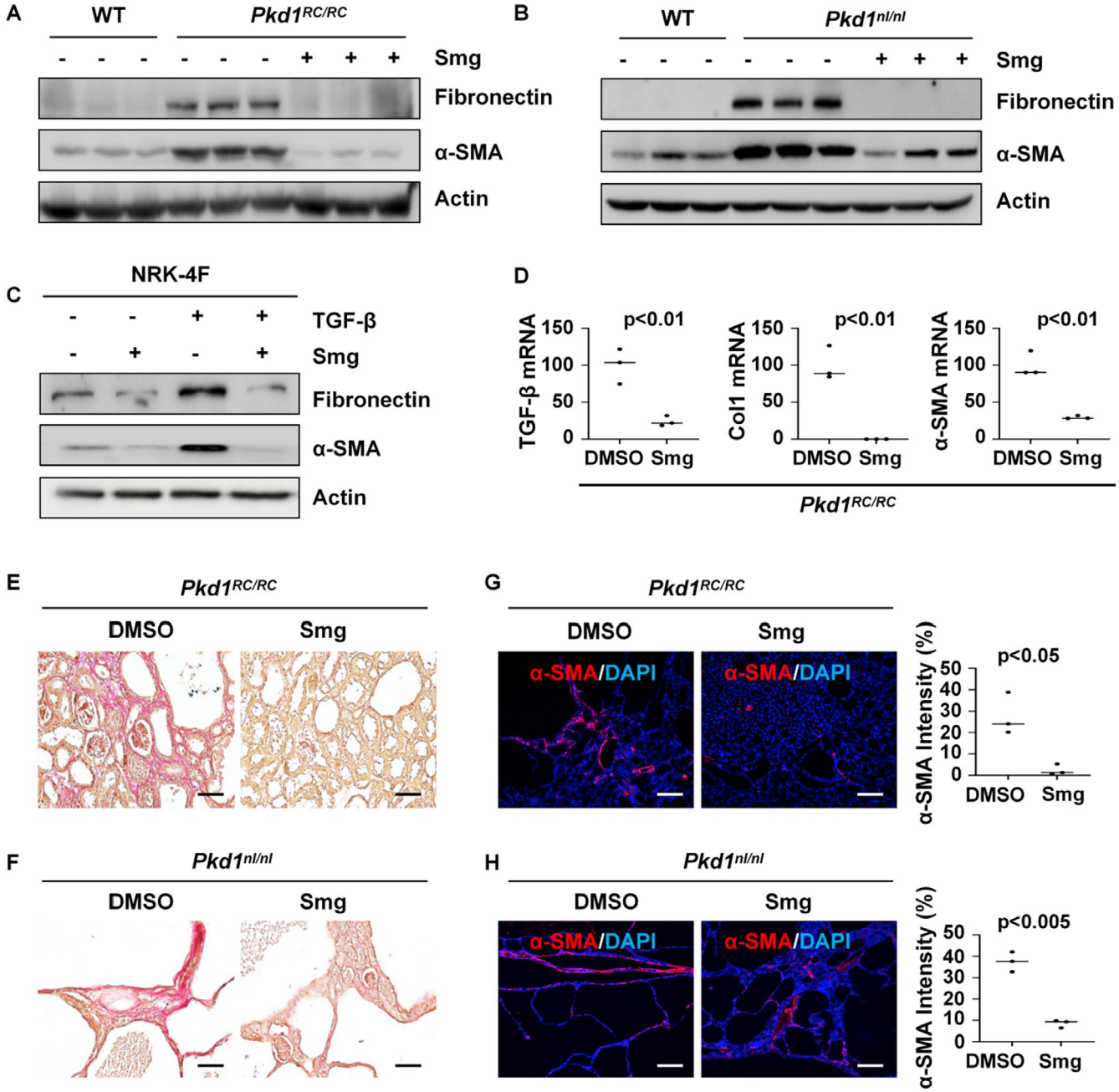

FIGURE 7 | Treatment with Smaglutide alleviates renal fibrosis in *Pkd1* mutant kidneys. (A) Western blot analysis of fibronectin and α-SMA expression in kidneys from PN91 $Pkd1^{RC/RC}$ mice treated with Semaglutide or vehicle. (B) Western blot analysis of fibronectin and α-SMA expression in kidneys from PN25 $Pkd1^{nl/nl}$ mice treated with Semaglutide or vehicle. (C) Western blot analysis of fibronectin and α-SMA expression in whole-cell lysates of rat kidney fibroblasts (NRK-49F) co-treated with TGF-β and Semaglutide or DMSO. (D) qRT-PCR analysis of TGF-β, collagen 1 and α-SMA mRNA expression in kidneys from PN91 $Pkd1^{RC/RC}$ mice treated with Semaglutide or vehicle. $p < 0.05$. All data were analyzed from three experiments. (E, F) Picrosirius red staining revealed reduced renal fibrosis in kidneys of PN91 $Pkd1^{RC/RC}$ mice (E) and in kidneys from PN25 $Pkd1^{nl/nl}$ mice (F) treated with Semaglutide compared to treated with vehicle. Scale bars: 50 μm. (G and H) Immunostaining of α-SMA expression in kidneys of PN91 $Pkd1^{RC/RC}$ mice (G) and in kidneys from PN25 $Pkd1^{nl/nl}$ mice (H) treated with Semaglutide compared to treated with vehicle. Scale bars: 100 μm. All statistical data are represented as mean ± SEM. Statistical analysis was performed using an unpaired two-tailed Student's *t* test.

in kidneys from *Pkd1*$^{RC/RC}$ mice treated with Smaglutide as examined with qRT-PCR analysis (Figure 7D). Notably, administration of Smaglutide decreased renal fibrosis as seen by a reduction of extracellular matrix deposition and a decrease in the expression of α-SMA in both *Pkd1*$^{RC/RC}$ and *Pkd1*$^{nl/nl}$ kidneys compared to that in control kidneys treated with vehicle as examined by picrosirius red staining (Figure 7E,F) and α-SMA staining (Figure 7G,H).

4 | Discussion

In recent years, GLP-1R medications have become a focus in biomedical research due to their innovative mechanisms, significant therapeutic efficacy, and broad development prospects. However, the role and mechanisms of GLP-1R signaling in ADPKD remain poorly understood. In this study, we define the role and mechanisms of GLP-1R and GLP-1RA in ADPKD. We show that the expression of GLP-1R is significantly downregulated in cystic kidneys, and pharmacological activation of GLP-1R with Semaglutide delays cyst growth through (1) a decrease of glucose uptake and ATP generation, (2) a normalization of mitochondrial morphology and function, (3) a decrease of PKD associated signaling pathways, including Rb, S6, and Stat3, leading to a decrease of *Pkd1* mutant renal epithelial cell proliferation, (4) an induction of *Pkd1* mutant renal epithelial cell death, (5) a decrease of the expression of cytokines and the recruitment of macrophages, (6) an induction of ketosis, and (7) an alleviation of renal fibrosis in *Pkd1* mutant mouse kidneys. This study not only addresses the mechanisms associated with GLP-1R signaling in the pathophysiology of ADPKD but also highlights the potential of GLP-1R agonists as a novel therapeutic strategy for ADPKD treatment.

The most remarkable value of this study is the link of GLP-1R signaling with metabolic dysregulation in ADPKD. GLP-1R, a GPCR, is critical for maintaining metabolic and renal homeostasis, which is known to exert protective effects in diabetic nephropathy by reducing oxidative stress and inflammation [53]. The observed downregulation of GLP-1R in cystic epithelial cells aligning with prior reports links GPCR dysfunction to ADPKD progression, particularly through dysregulated cAMP signaling [54]. Notably, GLP-1R agonists, (GLP-1RAs), such as Semaglutide, have shown renoprotective benefits in clinical trials [55–57]. We show that the reduction of GLP-1R expression may exacerbate the Warburg-like effect, a metabolic shift toward aerobic glycolysis, observed in cystic epithelia [35]. *Pkd1* mutant renal epithelial cells exhibit a hyperglycolytic phenotype, characterized by an elevation of glucose uptake and ATP production, a hallmark of PKD [36]. Treatment with Semaglutide could reverse this metabolic shift through a downregulation of the expression of glycolytic enzymes, including Hk1, Pkm2, Ldha and Ldhb, and an activation of AMPK, a master regulator of energy homeostasis [58]. AMPK activation inhibits mTORC1, a key driver of cyst growth, and promotes oxidative stress over glycolysis [59]. Semaglutide, as a modulator of AMPK-driven pathways, can restore the activity of GLP-1R to attenuate glucose uptake and ATP production in *Pkd1* mutant renal epithelial cells. However, the anti-cystic effects of Semaglutide are independent of the changes of blood glucose, highlighting a direct role of GLP-1R signaling in ADPKD pathogenesis.

Mitochondria are membrane-bound cell organelles that generate most of the chemical energy needed for cellular biochemical reactions [60]. The ability of Semaglutide to preserve mitochondrial morphology and function in *Pkd1* mutant kidneys represents a critical mechanistic breakthrough. Mitochondrial dysfunction, evidenced by a reduction in the expression of respiratory chain genes, including *mt-Nd6, mt-Col1, mt-Cytb*, and *mt-Rnr2*, and structural abnormalities, contribute to ADPKD progression [37, 43]. Excessive mitochondrial fission-fusion cycles are known to generate reactive oxygen species (ROS) and impair bioenergetic efficiency [61]. Treatment with Semaglutide could normalize the expression of mitochondrial respiratory chain genes, cristae morphology, and the abundance of mitochondria, mirroring the effects of AMPK activators to improve mitochondrial biogenesis and function in metabolic diseases [62]. The rescue of mitochondrial integrity may underpin the ability of Semaglutide in the control of ATP overproduction in ADPKD kidneys.

We also show a dual role of GLP-1R signaling in the regulation of proliferation and apoptosis in ADPKD kidneys. The deficiency of GLP-1R exacerbates cyst growth by impairing anti-proliferative and pro-survival pathways. Treatment with Semaglutide suppressed the phosphorylation and activation of Rb, S6, and Stat3, key PKD-associated pathways driving cystic cell proliferation [63], which might serve as a nodal point that links GLP-1R activation with metabolic and proliferative pathways. However, a direct modulator that regulates Semaglutide-mediated dephosphorylation of PKD-associated signaling pathways remains unknown, which needs to be further investigated. In addition, how Semaglutide induces apoptosis, a mechanism previously linked to GLP-1RA-mediated elimination of damaged cells [64], also needs to be elucidated.

Inflammation plays a crucial role in the development and progression of PKD, marked by an elevation of cytokines (e.g., TNF-a, MCP-1, etc.) and macrophage infiltration [65]. There is strong evidence indicating that semaglutide can modulate or reduce inflammatory processes [66–68]. The anti-inflammatory effects of Semaglutide are involved in two major mechanisms: reducing inflammatory cytokine levels and modifying immune system activity [69]. First, Semaglutide has been shown to suppress the release of pro-inflammatory cytokines, such as IL-6 and TNF-α, mediated by the NLRP3 inflammasome, a complex involved in regulating the innate immune system and inflammatory responses [70]. In addition, semaglutide can reduce inflammation signaling pathways, including p38 MAPK, c-Jun-NF-κB [71]. Second, Semaglutide can modulate immune system activity through various pathways. For example, semaglutide can activate GLP-1 receptors on endothelial and hematopoietic cells in mice, resulting in a reduction of inflammatory cytokines such as TNF-α, Abcg1, TGF-β1, Cd3g, and CCL-2 in hepatocytes [72]. Semaglutide can also decrease the recruitment or activity of immune cells [73]. It has been reported that semaglutide reduces leukocyte recruitment and rolling, decreases atherogenic plaque formation in mice, and suppresses the recruitment of cytotoxic $CD8^+$ T-cells into hepatocytes in an animal model of non-alcoholic steatohepatitis (NASH) [74]. In addition, Semaglutide can modulate immune system activity by reducing the proliferation of inflammatory cells [75]. Treatment with Semaglutide reduced macrophage recruitment and suppressed the expression

of TNF-a and MCP-1 via deactivation of NF-kB, which is aligned well with the known anti-inflammatory effects of Semaglutide.

Dietary interventions that induce a state of ketosis were found to inhibit disease progression in animal models of PKD [76]. It has been reported that time-restricted feeding and ketogenic diet inhibit proliferation and fibrosis in PKD kidneys in a rat model, and oral administration of the ketone β-hydroxybutyrate (BHB) in rats also strongly inhibits PKD progression, suggesting that cystic cells are metabolically inflexible and can be exploited by dietary interventions or supplementation with BHB [76]. In this study, we demonstrated that treatment with Semaglutide in delaying cyst growth is possibly through ketosis induction characterized by a rescue of serum BHB in ADPKD mice, supporting a novel mechanism for Semaglutide to execute its effect on delaying cyst growth in ADPKD.

Interstitial fibrosis is a hallmark of end-stage ADPKD [52]. GLP-1RAs have been shown to inhibit TGF-b mediated fibroblast activation in diabetic nephropathy [77]. The mechanisms of Semaglutide inhibit fibrosis include the inhibition of TGF-β signaling, the reduction of oxidative stress and inflammation, and the activation of AMPK [78]. Semaglutide inhibits TGF-b1-induced Smad2/3 phosphorylation, reducing the activation of fibroblasts and their differentiation into myofibroblasts [79]. In addition, Semaglutide can decrease cardiac fibrosis by preserving mitochondrial structure (e.g., reducing swelling and cristae disruption) and by promoting pyruvate entry into the tricarboxylic acid (TCA) cycle, which optimizes ATP production and mitigates energy deficiency in cardiomyocytes [53]. Semaglutide can also alleviate oxidative damage by changing mitochondrial structure and metabolism, and reducing reactive oxygen species (ROS) to exacerbate fibrosis [78]. Furthermore, Semaglutide can indirectly reduce fibrosis by lowering pro-inflammatory cytokines (e.g., TNF-α and IL-6) [79], resulting in a decrease of fibroblast activation [80]. Treatment with Semaglutide decreases the expression of fibrosis markers (fibronectin, a-SMA, Col1) and the deposition of extracellular matrix in *Pkd1* mutant mouse kidneys, likely by blunting the key fibrotic driver, TGF-b signaling [81], changing mitochondrial metabolism, and lowering pro-inflammatory cytokines in ADPKD kidneys. In sum, this study supports the idea that the anti-inflammation and anti-fibrotic effect of Semaglutide may synergize with its metabolic benefits to preserve renal function in ADPKD kidneys.

Author Contributions

J.W. performed most experiments and data analysis. A.S.C. performed some of the experiments and data analysis. T.W. helped in data analysis; P.C.H. and J.X.Z. helped in manuscript preparation. X.L. supervised the whole project, data analysis, and manuscript writing.

Acknowledgments

We thank Dr. Stefan Somlo for providing PH2 and PN24 cell lines through the George M. O'Brien Kidney Center at Yale University. We thank Dr. Dorien J.M. Peters at Leiden University Medical Center for providing *Pkd1*$^{nl/nl}$ mice. X.L. acknowledges support from NIH R01 DK129241 and NIH R01 DK126662 and DOD (Focused Program Award: PR221810). J.W. acknowledges support from Project of Hubei Province, WJ2025M005. A.S.C. acknowledges support from AHA, 24POST1242218.

Conflicts of Interest

The authors declare no conflicts of interest.

Data Availability Statement

The data that support the findings of this study are available in the Materials and Methods, Results, and/or Supporting Information of this article.

References

1. E. Cornec-Le Gall, A. Alam, and R. D. Perrone, "Autosomal Dominant Polycystic Kidney Disease," *Lancet* 393 (2019): 919–935.

2. M. Mahboob, P. Rout, S. W. Leslie, and S. R. A. Bokhari, "Autosomal Dominant Polycystic Kidney Disease," in *StatPearls* (Treasure Island (FL) Ineligible Companies. StatPearls Publishing LLC, 2025).

3. S. S. Jdiaa, R. A. Mustafa, and A. S. L. Yu, "Treatment of Autosomal-Dominant Polycystic Kidney Disease," *American Journal of Kidney Diseases* 85 (2024): 491–500.

4. V. E. Torres, A. B. Chapman, O. Devuyst, et al., "Tolvaptan in Later-Stage Autosomal Dominant Polycystic Kidney Disease," *New England Journal of Medicine* 377 (2017): 1930–1942.

5. F. M. Gribble and F. Reimann, "Metabolic Messengers: Glucagon-Like Peptide 1," *Nature Metabolism* 3 (2021): 142–148.

6. M. K. Klausen, M. Thomsen, G. Wortwein, and A. Fink-Jensen, "The Role of Glucagon-Like Peptide 1 (GLP-1) in Addictive Disorders," *British Journal of Pharmacology* 179 (2022): 625–641.

7. M. P. Gilbert and R. E. Pratley, "GLP-1 Analogs and DPP-4 Inhibitors in Type 2 Diabetes Therapy: Review of Head-To-Head Clinical Trials," *Frontiers in Endocrinology* 11 (2020): 178.

8. J. H. Yu, S. Y. Park, D. Y. Lee, N. H. Kim, and J. A. Seo, "GLP-1 Receptor Agonists in Diabetic Kidney Disease: Current Evidence and Future Directions," *Kidney Research and Clinical Practice* 41 (2022): 136–149.

9. C. F. Deacon, A. H. Johnsen, and J. J. Holst, "Degradation of Glucagon-Like Peptide-1 by Human Plasma in Vitro Yields an N-Terminally Truncated Peptide That Is a Major Endogenous Metabolite in Vivo," *Journal of Clinical Endocrinology and Metabolism* 80 (1995): 952–957.

10. D. J. Drucker and M. A. Nauck, "The Incretin System: Glucagon-Like Peptide-1 Receptor Agonists and Dipeptidyl Peptidase-4 Inhibitors in Type 2 Diabetes," *Lancet* 368 (2006): 1696–1705.

11. M. A. Nauck and J. J. Meier, "Incretin Hormones: Their Role in Health and Disease," *Diabetes, Obesity & Metabolism* 20, no. Suppl 1 (2018): 5–21.

12. D. J. Drucker, "The Biology of Incretin Hormones," *Cell Metabolism* 3 (2006): 153–165.

13. D. Xu, A. Nair, C. Sigston, et al., "Potential Roles of Glucagon-Like Peptide 1 Receptor Agonists (GLP-1 RAs) in Nondiabetic Populations," *Cardiovascular Therapeutics* 2022 (2022): 6820377.

14. J. P. Ferreira, A. Sharma, J. Butler, et al., "Glucagon-Like Peptide-1 Receptor Agonists Across the Spectrum of Heart Failure," *Journal of Clinical Endocrinology and Metabolism* 109 (2023): 4–9.

15. S. C. Palmer, B. Tendal, R. A. Mustafa, et al., "Sodium-Glucose Cotransporter Protein-2 (SGLT-2) Inhibitors and Glucagon-Like Peptide-1 (GLP-1) Receptor Agonists for Type 2 Diabetes: Systematic Review and Network Meta-Analysis of Randomised Controlled Trials," *BMJ (Clinical Research Ed)* 372 (2021): m4573.

16. K. C. Sourris, Y. Ding, S. S. Maxwell, et al., "Glucagon-Like Peptide-1 Receptor Signaling Modifies the Extent of Diabetic Kidney Disease Through Dampening the Receptor for Advanced Glycation End Products–Induced Inflammation," *Kidney International* 105 (2024): 132–149.

17. T. P. Vahl, B. W. Paty, B. D. Fuller, R. L. Prigeon, and D. A. D'Alessio, "Effects of GLP-1-(7-36)NH2, GLP-1-(7-37), and GLP-1- (9-36)NH2 on Intravenous Glucose Tolerance and Glucose-Induced Insulin Secretion in Healthy Humans," *Journal of Clinical Endocrinology and Metabolism* 88 (2003): 1772–1779.

18. M. A. Nauck, D. R. Quast, J. Wefers, and J. J. Meier, "GLP-1 Receptor Agonists in the Treatment of Type 2 Diabetes - State-Of-The-Art," *Molecular Metabolism* 46 (2021): 101102.

19. E. H. Hu, M. L. Tsai, Y. Lin, T. S. Chou, and T. H. Chen, "A Review and Meta-Analysis of the Safety and Efficacy of Using Glucagon-Like Peptide-1 Receptor Agonists," *Medicina (Kaunas, Lithuania)* 60 (2024): 357.

20. N. R. Gandasi, R. Gao, L. Kothegala, et al., "GLP-1 Metabolite GLP-1(9-36) is a Systemic Inhibitor of Mouse and Human Pancreatic Islet Glucagon Secretion," *Diabetologia* 67 (2024): 528–546.

21. X. Zhou, L. X. Fan, W. E. Sweeney, Jr., J. M. Denu, E. D. Avner, and X. Li, "Sirtuin 1 Inhibition Delays Cyst Formation in Autosomal-Dominant Polycystic Kidney Disease," *Journal of Clinical Investigation* 123 (2013): 3084–3098.

22. F. Wei, A. Karihaloo, Z. Yu, et al., "Neutrophil Gelatinase-Associated Lipocalin Suppresses Cyst Growth by Pkd1 Null Cells in Vitro and in Vivo," *Kidney International* 74 (2008): 1310–1318.

23. K. Hopp, C. J. Ward, C. J. Hommerding, et al., "Functional Polycystin-1 Dosage Governs Autosomal Dominant Polycystic Kidney Disease Severity," *Journal of Clinical Investigation* 122 (2012): 4257–4273.

24. I. S. van Lantinga- Leeuwen, J. G. Dauwerse, H. J. Baelde, et al., "Lowering of Pkd1 Expression Is Sufficient to Cause Polycystic Kidney Disease," *Human Molecular Genetics* 13 (2004): 3069–3077.

25. M. H. Shihan, S. G. Novo, S. J. Le Marchand, Y. Wang, and M. K. Duncan, "A Simple Method for Quantitating Confocal Fluorescent Images," *Biochemistry and Biophysics Reports* 25 (2021): 100916.

26. J. Arroyo, D. Escobar-Zarate, H. H. Wells, et al., "The Genetic Background Significantly Impacts the Severity of Kidney Cystic Disease in the Pkd1(RC/RC) Mouse Model of Autosomal Dominant Polycystic Kidney Disease," *Kidney International* 99 (2021): 1392–1407.

27. H. Happé, A. M. van der Wal, D. C. Salvatori, et al., "Cyst Expansion and Regression in a Mouse Model of Polycystic Kidney Disease," *Kidney International* 83 (2013): 1099–1108.

28. L. E. M. Cardoso, T. S. Marinho, F. F. Martins, M. B. Aguila, and C. A. Mandarim-de-Lacerda, "Treatment With Semaglutide, a GLP-1 Receptor Agonist, Improves Extracellular Matrix Remodeling in the Pancreatic Islet of Diet-Induced Obese Mice," *Life Sciences* 319 (2023): 121502.

29. L. Poupon-Bejuit, M. P. Hughes, W. Liu, et al., "A GLP1 Receptor Agonist Diabetes Drug Ameliorates Neurodegeneration in a Mouse Model of Infantile Neurometabolic Disease," *Scientific Reports* 12 (2022): 13825.

30. W. Qin, J. Yang, C. Deng, Q. Ruan, and K. Duan, "Efficacy and Safety of Semaglutide 2.4 Mg for Weight Loss in Overweight or Obese Adults Without Diabetes: An Updated Systematic Review and Meta-Analysis Including the 2-Year STEP 5 Trial," *Diabetes, Obesity & Metabolism* 26 (2024): 911–923.

31. J. P. H. Wilding, R. L. Batterham, S. Calanna, et al., "Once-Weekly Semaglutide in Adults With Overweight or Obesity," *New England Journal of Medicine* 384 (2021): 989–1002.

32. H. Yao, A. Zhang, D. Li, et al., "Comparative Effectiveness of GLP-1 Receptor Agonists on Glycaemic Control, Body Weight, and Lipid Profile for Type 2 Diabetes: Systematic Review and Network Meta-Analysis," *BMJ (Clinical Research Ed)* 384 (2024): e076410.

33. N. C. Bergmann, M. J. Davies, I. Lingvay, and F. K. Knop, "Semaglutide for the Treatment of Overweight and Obesity: A Review," *Diabetes, Obesity & Metabolism* 25 (2023): 18–35.

34. I. Bakaj and A. Pocai, "Metabolism-Based Approaches for Autosomal Dominant Polycystic Kidney Disease," *Frontiers in Molecular Biosciences* 10 (2023): 1126055.

35. L. Chen, X. Zhou, L. X. Fan, et al., "Macrophage Migration Inhibitory Factor Promotes Cyst Growth in Polycystic Kidney Disease," *Journal of Clinical Investigation* 125 (2015): 2399–2412.

36. I. Rowe, M. Chiaravalli, V. Mannella, et al., "Defective Glucose Metabolism in Polycystic Kidney Disease Identifies a New Therapeutic Strategy," *Nature Medicine* 19 (2013): 488–493.

37. V. Padovano, C. Podrini, A. Boletta, and M. J. Caplan, "Metabolism and Mitochondria in Polycystic Kidney Disease Research and Therapy," *Nature Reviews Nephrology* 14 (2018): 678–687.

38. C. Stone, D. D. Harris, M. Broadwin, et al., "Semaglutide Improves Myocardial Perfusion and Performance in a Large Animal Model of Coronary Artery Disease," *Arteriosclerosis, Thrombosis, and Vascular Biology* 45 (2025): 285–297.

39. T. Doke and K. Susztak, "The Multifaceted Role of Kidney Tubule Mitochondrial Dysfunction in Kidney Disease Development," *Trends in Cell Biology* 32 (2022): 841–853.

40. H. C. Lee and Y. H. Wei, "Mitochondrial Role in Life and Death of the Cell," *Journal of Biomedical Science* 7 (2000): 2–15.

41. Y. Liu, K. Xu, Y. Xiang, et al., "Role of MCP-1 as an Inflammatory Biomarker in Nephropathy," *Frontiers in Immunology* 14 (2023): 1303076.

42. S. Pieter, B. Bert, M. Djalila, M. Isabelle, and V. Rudi, "#2396 the Potential of Human-Derived Macrophages to Study Autosomal Dominant Polycystic Kidney Disease (ADPKD)," *Nephrology, Dialysis, Transplantation* Supplement_1 (2024), https://doi.org/10.1093/ndt/gfae069.007.

43. J. Wu, S. Cheng, G. Lee, E. Agborbesong, X. Li, and X. Zhou, "STING Promotes the Progression of ADPKD by Regulating Mitochondrial Function, Inflammation, Fibrosis, and Apoptosis," *Biomolecules* 14 (2024): 1215.

44. M. Mussbacher, M. Derler, J. Basílio, and J. A. Schmid, "NF-κB in Monocytes and Macrophages – An Inflammatory Master Regulator in Multitalented Immune Cells," *Frontiers in Immunology* 14 (2023): 1134661.

45. L. Pickel, I. A. Iliuta, J. Scholey, Y. Pei, and H. K. Sung, "Dietary Interventions in Autosomal Dominant Polycystic Kidney Disease," *Advances in Nutrition (Bethesda, md)* 13 (2022): 652–666.

46. A. K. Lee, D. H. Kim, E. Bang, Y. J. Choi, and H. Y. Chung, "β-Hydroxybutyrate Suppresses Lipid Accumulation in Aged Liver Through GPR109A-Mediated Signaling," *Aging and Disease* 11 (2020): 777–790.

47. J. Ngo, D. W. Choi, I. A. Stanley, et al., "Mitochondrial Morphology Controls Fatty Acid Utilization by Changing CPT1 Sensitivity to Malonyl-CoA," *EMBO Journal* 42 (2023): e111901.

48. K. Bartlett and S. Eaton, "Mitochondrial Beta-Oxidation," *European Journal of Biochemistry* 271 (2004): 462–469.

49. S. Yamauchi, Y. Sugiura, J. Yamaguchi, et al., "Mitochondrial Fatty Acid Oxidation Drives Senescence," *Science Advances* 10 (2024): eado5887.

50. V. Miguel, J. Tituaña, J. I. Herrero, et al., "Renal Tubule Cpt1a Overexpression Protects From Kidney Fibrosis by Restoring Mitochondrial Homeostasis," *Journal of Clinical Investigation* 131 (2021): e140695.

51. Y. H. Zhang, L. Bin, Q. Meng, et al., "ACOX1 Deficiency-Induced Lipid Metabolic Disorder Facilitates Chronic Interstitial Fibrosis Development in Renal Allografts," *Pharmacological Research* 201 (2024): 107105.

52. Y. Zhang, G. Reif, and D. P. Wallace, "Extracellular Matrix, Integrins, and Focal Adhesion Signaling in Polycystic Kidney Disease," *Cellular Signalling* 72 (2020): 109646.

53. D. J. Drucker, "The Cardiovascular Biology of Glucagon-Like Peptide-1," *Cell Metabolism* 24 (2016): 15–30.

54. "Global, Regional, and National Burden of Chronic Kidney Disease, 1990-2017: A Systematic Analysis for the Global Burden of Disease Study 2017," *Lancet* 395 (2020): 709–733.

55. M. H. A. Muskiet, L. Tonneijck, M. M. Smits, et al., "GLP-1 and the Kidney: From Physiology to Pharmacology and Outcomes in Diabetes," *Nature Reviews. Nephrology* 13 (2017): 605–628.

56. K. R. Tuttle, H. Bosch-Traberg, D. Z. I. Cherney, et al., "Post Hoc Analysis of SUSTAIN 6 and PIONEER 6 Trials Suggests That People With Type 2 Diabetes at High Cardiovascular Risk Treated With Semaglutide Experience More Stable Kidney Function Compared With Placebo," *Kidney International* 103 (2023): 772–781.

57. A. M. Shaman, S. C. Bain, G. L. Bakris, et al., "Effect of the Glucagon-Like Peptide-1 Receptor Agonists Semaglutide and Liraglutide on Kidney Outcomes in Patients With Type 2 Diabetes: Pooled Analysis of SUSTAIN 6 and LEADER," *Circulation* 145 (2022): 575–585.

58. L. K. Townsend and G. R. Steinberg, "AMPK and the Endocrine Control of Metabolism," *Endocrine Reviews* 44 (2023): 910–933.

59. D. G. Hardie, F. A. Ross, and S. A. Hawley, "AMPK: A Nutrient and Energy Sensor That Maintains Energy Homeostasis," *Nature Reviews Molecular Cell Biology* 13 (2012): 251–262.

60. L. D. Osellame, T. S. Blacker, and M. R. Duchen, "Cellular and Molecular Mechanisms of Mitochondrial Function," *Best Practice & Research Clinical Endocrinology & Metabolism* 26 (2012): 711–723.

61. D. C. Chan, "Mitochondrial Dynamics and Its Involvement in Disease," *Annual Review of Pathology* 15 (2020): 235–259.

62. H. Zong, J. M. Ren, L. H. Young, et al., "AMP Kinase Is Required for Mitochondrial Biogenesis in Skeletal Muscle in Response to Chronic Energy Deprivation," *Proceedings of the National Academy of Sciences of the United States of America* 99 (2002): 15983–15987.

63. J. M. Shillingford, N. S. Murcia, C. H. Larson, et al., "The mTOR Pathway Is Regulated by Polycystin-1, and Its Inhibition Reverses Renal Cystogenesis in Polycystic Kidney Disease," *Proceedings of the National Academy of Sciences of the United States of America* 103 (2006): 5466–5471.

64. Y. S. Lee and H. S. Jun, "Anti-Inflammatory Effects of GLP-1-Based Therapies Beyond Glucose Control," *Mediators of Inflammation* 2016 (2016): 3094642.

65. A. Karihaloo, F. Koraishy, S. C. Huen, et al., "Macrophages Promote Cyst Growth in Polycystic Kidney Disease," *Journal of the American Society of Nephrology* 22 (2011): 1809–1814.

66. S. A. Tan and L. Tan, "LIRAGLUTIDE and SEMAGLUTIDE Attenuate Inflammatory Cytokines Interferon-Gamma, Tumor Necrosis Factor-Alpha, and INTERLEUKIN-6: Possible Mechanism of Decreasing Cardiovascular Risk in Diabetes Mellitus," *Journal of the American College of Cardiology* 73 (2019): 1866.

67. I. Reppo, M. Jakobson, and V. Volke, "Effects of Semaglutide and Empagliflozin on Inflammatory Markers in Patients With Type 2 Diabetes," *International Journal of Molecular Sciences* 24 (2023): 5714.

68. A. Mima, S. Kidooka, T. Nakamoto, et al., "Effects of Oral Semaglutide on Renal Function in Diabetic Kidney Disease: A Short-Term Clinical Study," *In Vivo (Athens, Greece)* 38 (2024): 308–312.

69. G. Bendotti, L. Montefusco, M. E. Lunati, et al., "The Anti-Inflammatory and Immunological Properties of GLP-1 Receptor Agonists," *Pharmacological Research* 182 (2022): 106320.

70. L. Wang, J. Ding, C. Zhu, et al., "Semaglutide Attenuates Seizure Severity and Ameliorates Cognitive Dysfunction by Blocking the NLR Family Pyrin Domain Containing 3 Inflammasome in Pentylenetetrazole-Kindled Mice," *International Journal of Molecular Medicine* 48 (2021): 219.

71. X. Yang, P. Feng, X. Zhang, et al., "The Diabetes Drug Semaglutide Reduces Infarct Size, Inflammation, and Apoptosis, and Normalizes Neurogenesis in a Rat Model of Stroke," *Neuropharmacology* 158 (2019): 107748.

72. B. A. McLean, C. K. Wong, K. D. Kaur, R. J. Seeley, and D. J. Drucker, "Differential Importance of Endothelial and Hematopoietic Cell GLP-1Rs for Cardiometabolic Versus Hepatic Actions of Semaglutide," *JCI Insight* 6 (2021): e153732.

73. G. Rakipovski, B. Rolin, J. Nøhr, et al., "The GLP-1 Analogs Liraglutide and Semaglutide Reduce Atherosclerosis in ApoE(−/−) and LDLr(−/−) Mice by a Mechanism That Includes Inflammatory Pathways," *JACC Basic to Translational Science* 3 (2018): 844–857.

74. W. Latif, K. J. Lambrinos, P. Patel, and R. Rodriguez, "Compare and Contrast the Glucagon-Like Peptide-1 Receptor Agonists (GLP1RAs)," in *StatPearls*, vol. 40 (Treasure Island (FL) Ineligible Companies, StatPearls Publishing LLC, 2025), 137.

75. X. Pan, L. Yang, S. Wang, Y. Liu, L. Yue, and S. Chen, "Semaglutide Ameliorates Obesity-Induced Cardiac Inflammation and Oxidative Stress Mediated via Reduction of Neutrophil Cxcl2, S100a8, and S100a9 Expression," *Molecular and Cellular Biochemistry* 479 (2024): 1133–1147.

76. J. A. Torres, S. L. Kruger, C. Broderick, et al., "Ketosis Ameliorates Renal Cyst Growth in Polycystic Kidney Disease," *Cell Metabolism* 30 (2019): 1007–1023.e1005.

77. R. Kodera, K. Shikata, H. U. Kataoka, et al., "Glucagon-Like Peptide-1 Receptor Agonist Ameliorates Renal Injury Through Its Anti-Inflammatory Action Without Lowering Blood Glucose Level in a Rat Model of Type 1 Diabetes," *Diabetologia* 54 (2011): 965–978.

78. Y. L. Ma, C. Y. Kong, Z. Guo, et al., "Semaglutide Ameliorates Cardiac Remodeling in Male Mice by Optimizing Energy Substrate Utilization Through the Creb5/NR4a1 Axis," *Nature Communications* 15 (2024): 4757.

79. Y. Tashiro, K. Sato, T. Watanabe, et al., "A Glucagon-Like Peptide-1 Analog Liraglutide Suppresses Macrophage Foam Cell Formation and Atherosclerosis," *Peptides* 54 (2014): 19–26.

80. R. Bignold and J. R. Johnson, "Effects of Cytokine Signaling Inhibition on Inflammation-Driven Tissue Remodeling," *Current Research in Pharmacology and Drug Discovery* 2 (2021): 100023.

81. M. Zeisberg and E. G. Neilson, "Mechanisms of Tubulointerstitial Fibrosis," *Journal of the American Society of Nephrology* 21 (2010): 1819–1834.

Supporting Information

Additional supporting information can be found online in the Supporting Information section. **Table S1:** The sequences of all primers used for qRT-PCR. **Data S2:** fsb270944-sup-0002-DataS2.docx.